The 2010 IEEE/RSJ International Conference on
Intelligent Robots and Systems
October 18-22, 2010, Taipei, Taiwan

# Biped Walking Stabilization Based on Linear Inverted Pendulum Tracking

Shuuji Kajita, Mitsuharu Morisawa, Kanako Miura, Shin'ichiro Nakaoka,
Kensuke Harada, Kenji Kaneko, Fumio Kanehiro and Kazuhito Yokoi

*Abstract*— **A novel framework of biped walking stabilization control is introduced. The target robot is a 42 DOF humanoid robot HRP-4C which has a body dimensions close to the average Japanese female. We develop a body posture controller and foot force controllers on the joint position servo of the robot. By applying this posture/force control, we can regard the robot system as a simple linear inverted pendulum with ZMP delay. After a preliminary experiment to confirm the linear dynamics, we design a tracking controller for walking stabilization. It is evaluated in the experiments of HRP-4C walking and turning on a lab floor. The robot can also perform an outdoor walk on an uneven pavement.**

## I. INTRODUCTION

The premise of Zero-Moment Point (ZMP) [1] is that dynamic biped walking control can be decomposed into two parts, a walking pattern generation and a stabilization around it. In this paper, we discuss the latter part.

There are standpoints which the premise of ZMP is wrong, for walking pattern and stabilization are deeply coupled. In this view, a system has no explicit *walking pattern* as a function of time but has *basin of attraction* [2]–[4]. This is very interesting concept, but let us leave it for the future discussion.

On the other hand, there are real-time walking pattern generators which has a function of stabilizer [5], [6]. They change the step length or the step period in a time span of a few seconds, while a stabilizer we mentioned first works in a time span of a few milli-seconds. Both systems can co-exist and can enhance each other.

So let us discuss a stabilizer which works around a given walking pattern. It is still important, for example, when a robot dances with other performers, it is necessary to track the pre-determined trajectory as close as possible. Yamaguchi, Takanishi and Kato proposed a foot mechanism with shock absorbing material to realize reliable biped dynamic walking [7]. Hirai et al. developed a humanoid robot P2 which surprised world robotics researchers by its beautiful biped walking. Their stabilizer did intensively used the ZMP [8]. Nagasaka et al. [9] developed another ZMP based stabilizer for a biped robot. Choi et al. introduced a similar controller with clear formalization and stability proof by Lyapunov method [10]. Qiang et al. proposed real-time posture and ZMP control to stabilize a simulated biped robot [11]. Kim and Oh developed an effective stabilizer using an ankle torque feedback to regulate the structural vibration [12]. Another effective method which uses hybrid position/force control was proposed by Buschmann et al. [13]

Most of these methods can stabilize a biped robot on flat floors, but not on unknown uneven ground. To solve this, Kang et al. introduced specially designed foot mechanism for uneven terrain walking [14]. Nishiwaki and Kagami designed a walking pattern generator which changes the future ZMP to maintain the instantaneous balance [15]. However, the first method requires a special hardware and the second method does not keep the given trajectory.

Fig. 1. Walking on a pavement

In this paper, we propose a novel walking stabilization for a robot with conventional foot mechanism. Although our algorithm gives only a small modification along a pre-determined trajectory, it can show a certain robustness, i.e. our humanoid robot can walk on an outdoor pavement(Fig.1). The rest of this paper is organized as follows. In Section II, we introduce the target walking robot and the basic structure of our controller. In Section III, we explain the middle level of the controller which controls the body posture and the foot force/torque to realize a specified ZMP reference. In Section VI, we design a CoM/ZMP tracking controller based on the

This work was supported by AIST and CREST.

S. Kajita, M.Morisawa, K.Miura, S.Nakaoka, K.Harada, K.Kaneko, F.Kanehiro and K.Yokoi are in Humanoid Robotics Group, Intelligent systems institute, AIST, Tsukuba, Ibaraki, 305-8568, Japan s.kajita@aist.go.jp

S.Kajita and F.Kanehiro are in Japan Science and Technology Agency, CREST, 5, Sanbancho, Chiyoda-ku, Tokyo, 102-0075, Japan

linear inverted pendulum dynamics which emerges by the middle level control. In Section V, the experimental results of the robot with the proposed controller are shown. We conclude and address the future remarks in Section VI.

## II. Robot and Control

### A. Cybernetic human HRP-4C

The target robot for our control is Cybernetic human HRP-4C shown in Fig.1. It is a humanoid robot of 158cm height, 43kg weight and total 42 degrees of freedom (DOF). The body was designed to have close dimensions of the average Japanese young female [16]. To control the whole body motion, the robot body is equipped with a PCI-104 CPU board with Pentium M 1.6GHz. As a dependable real-time operating system, we installed ART-Linux 2.6 which ensures accurate cyclic execution of our control program [17], [18].

### B. Walking pattern

A walking pattern contains desired value of joint angles, body posture and ZMP for every control cycle (5ms). It can be generated analytically [19] or based on motion capturing [20].

### C. Controller overview

Figure 2 illustrates an overview of the stabilizer. The controller consists of three layers as follows.

Servo control layer
: This layer handles the sensors and actuators of the robot. It contains PID joint servo controllers and a Kalman filter to estimate the body posture from the angular velocity and the acceleration measured by the rate gyros and the G-sensors respectively.

Posture/Force control layer
: This layer takes care of the whole robot geometry to control the body posture, the foot torques and the foot forces. Its details are explained in Section III.

CoM/ZMP control layer
: This layer takes care of the CoM and ZMP of the robot. Its details are explained in Section IV.

## III. Posture/Force control layer

### A. Frames for control

Figure 3 shows the block diagram of the posture/force control layer. In every control cycle, the body posture, the joint angles and the walking pattern are converted into the spatial geometry of the robot by using forward kinematics. The results are the following position vectors and rotation matrices.

| | |
|---|---|
| $\boldsymbol{p}_R, \boldsymbol{R}_R$ | right foot position/orientation |
| $\boldsymbol{p}_L, \boldsymbol{R}_L$ | left foot position/orientation |
| $\boldsymbol{p}_B, \boldsymbol{R}_B$ | pelvis link position/orientaion |
| $\boldsymbol{R}_C$ | chest link orientation |

Note that the position of the chest link is not used since it can be determined from the chest orientation. For a frame

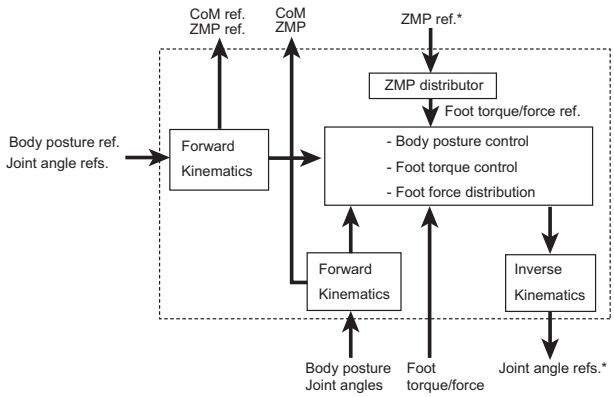


Fig. 3. Information flow in the posture/force control layer

calculated from the walking pattern we add a superscript $d$(Fig.4).

Our control algorithms explained in the following subsections are implemented to modify these reference frames in Cartesian space. At the end of each control cycle, the modified reference frames are converted into the joint angle reference by inverse kinematics. By this way, we can build a versatile controller independent from a specific mechanism.

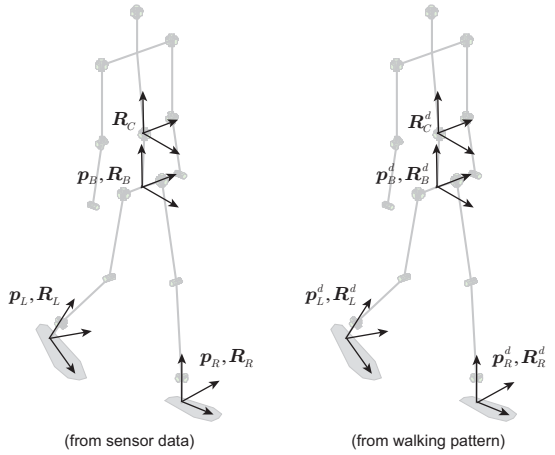


Fig. 4. Frames for stabilization control

### B. Chest posture control

The chest posture controller calculates additional rotation to let the chest frame follows the walking pattern. With current roll and pitch angle of chest frame $(\phi_C, \theta_C)$ and its reference $(\phi_C^d, \theta_C^d)$, we calculate angles for modification $(\Delta\phi_C, \Delta\theta_C)$ by

$$\Delta\dot{\phi}_C = k_C(\phi_C^d - \phi_C) - \frac{1}{T_C}\Delta\phi_C \quad (1)$$

$$\Delta\dot{\theta}_C = k_C(\theta_C^d - \theta_C) - \frac{1}{T_C}\Delta\theta_C, \quad (2)$$

where $k_C$ is a posture feedback gain and $T_C$ is a time constant to retrieve neutral points. These angles for modification

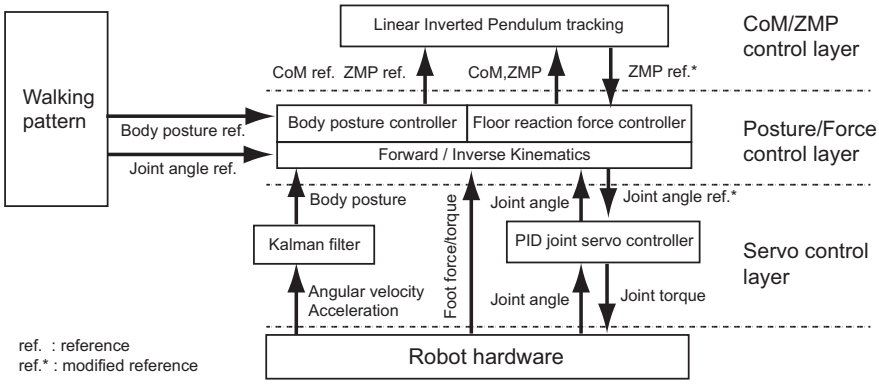


Fig. 2. Hierachical control structure

are transformed into the desired chest frame $\boldsymbol{R}_C^{d*}$ by using the following equation,

$$\boldsymbol{R}_C^{d*} = \boldsymbol{R}_C^d \boldsymbol{R}_{rpy}(\Delta\phi_C, \Delta\theta_C, 0) \tag{3}$$

where $\boldsymbol{R}_{rpy}(\cdot)$ calculates a rotation matrix with given roll-pitch-yaw angles. The superscript $d*$ indicates a modified reference value or frame.

### C. ZMP distributor

The ZMP distributor converts reference ZMP into target forces and torques for the foot force controller. In single support phase, or in double support phase whose reference ZMP exists within either one of the foot polygon, we can easily calculate them.

$$\boldsymbol{f}_R^d = -\alpha M\boldsymbol{g} \tag{4}$$
$$\boldsymbol{f}_L^d = -(1-\alpha)M\boldsymbol{g} \tag{5}$$
$$\boldsymbol{\tau}_i^d = (\boldsymbol{p}_i - \boldsymbol{p}_{zmp}^d) \times \boldsymbol{f}_i^d \quad (i = R, L) \tag{6}$$

where $\alpha$ is 1 when the ZMP is in the right foot polygon and $\alpha = 0$ when the ZMP is in the left foot polygon. $M$ and $\boldsymbol{g}$ are the robot mass and gravity acceleration vector, respectively.

During double support phase whose reference ZMP exists in neither left or right foot polygon as shown in Fig.5, we determine the force/torque distribution by a simple heuristics[1].

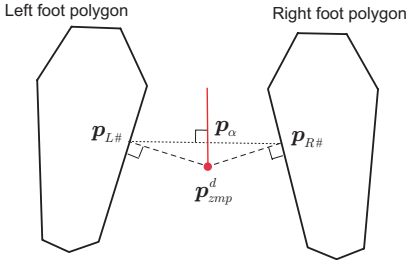


Fig. 5. ZMP distribution

[1]A different algorithm for the same purpose was proposed by Hyon for balancing control of his humanoid robot whose joint is torque controlled [21]

First, we draw a perpendicular line from the ZMP onto the foot polygons and determine the closest point $\boldsymbol{p}_{R\#}$ and $\boldsymbol{p}_{L\#}$. Also we define a point $\boldsymbol{p}_\alpha$ on the line $\boldsymbol{p}_{R\#}\boldsymbol{p}_{L\#}$ so that $\boldsymbol{p}_{zmp}^d\boldsymbol{p}_\alpha$ becomes perpendicular to the line. Force distribution ratio is determined by these points.

$$\alpha = \frac{|\boldsymbol{p}_\alpha - \boldsymbol{p}_{L\#}|}{|\boldsymbol{p}_{L\#} - \boldsymbol{p}_{R\#}|} \tag{7}$$

The target force can be obtained by (4) and (5) with this $\alpha$.

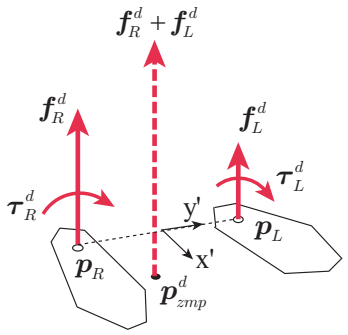


Fig. 6. ZMP, floor force and foot torque

Fig.6 illustrates the foot force/torque and ZMP. Since the moment created by the feet must be zero around the ZMP, we have

$$(\boldsymbol{p}_R - \boldsymbol{p}_{zmp}) \times \boldsymbol{f}_R^d + (\boldsymbol{p}_L - \boldsymbol{p}_{zmp}) \times \boldsymbol{f}_L^d + \boldsymbol{\tau}_R^d + \boldsymbol{\tau}_L^d = 0. \tag{8}$$

Thus we can determine the sum of torques of both feet.

$$\begin{aligned} \boldsymbol{\tau}_R^d + \boldsymbol{\tau}_L^d &= -(\boldsymbol{p}_R - \boldsymbol{p}_{zmp}) \times \boldsymbol{f}_R^d - (\boldsymbol{p}_L - \boldsymbol{p}_{zmp}) \times \boldsymbol{f}_L^d \\ &=: \boldsymbol{\tau}_0 \end{aligned} \tag{9}$$

We define a local x'y'-frame whose y' axis directs the left ankle from the right ankle (see Fig.6) and the torque $\boldsymbol{\tau}_0$ is

distributed by the following rules.

$$\tau_{Ry'} = \alpha\tau_{0y'} \quad (10)$$

$$\tau_{Ly'} = (1-\alpha)\tau_{0y'} \quad (11)$$

$$\tau_{Rx'} = \begin{cases} \tau_{0x'} & (\text{if } \tau_{0x'} < 0) \\ 0 & (\text{else}) \end{cases} \quad (12)$$

$$\tau_{Lx'} = \begin{cases} 0 & (\text{if } \tau_{0x'} < 0) \\ \tau_{0x'} & (\text{else}) \end{cases} \quad (13)$$

### D. Foot torque control

The foot torque controller modifies foot rotation to realize the foot reference torque calculated by the ZMP distributor.

We use the following damping controller to realize given foot torque $\tau^d$.

$$\dot{\delta} = D^{-1}(\tau^d - \tau) - \frac{1}{T}\delta, \quad (14)$$

where $D$ is damping gain. $T$ is a time constant to retrieve the neutral point when the foot is in the air at swing phase.

Let us define a function $damping()$ which returns a control variable $\delta$ for the given torque measurement and reference by (14). The foot reference frame is modified to control x and y component of the foot torque.

$$\boldsymbol{R}_i^{d*} = \boldsymbol{R}_i^d \boldsymbol{R}_{rpy}(\Delta\phi_i, \Delta\theta_i, 0) \quad (i = R, L) \quad (15)$$

$$\Delta\phi_i := damping(\tau_{ix}^{d*}, \tau_{ix}) \quad (16)$$

$$\Delta\theta_i := damping(\tau_{iy}^{d*}, \tau_{iy}) \quad (17)$$

### E. Foot force difference control

To realize the desired foot force calculated in III-C, we designed a controller which regulates the difference of the vertical foot forces during double support phase.

$$z_{ctrl} = damping(f_{Lz}^d - f_{Rz}^d, f_{Lz} - f_{Rz}) \quad (18)$$

By this control law, relative foot elevation $z_{ctrl}$ is adjusted to realize the target $f_{Lz}^d - f_{Rz}^d$. Fig. 7(a) shows a method to realize $z_{ctrl}$ in which each ankle height is changed as following.

$$p_{Rz}^{d*} = p_{Rz}^d + 0.5 z_{ctrl} \quad (19)$$

$$p_{Lz}^{d*} = p_{Lz}^d - 0.5 z_{ctrl} \quad (20)$$

For this modification, we need a walking pattern with knee bending at all times. Moreover, even for a walking pattern containing a moment of almost stretched knees, the control creates an undesirably high joint speed due to the singularity.

Fig. 7(b) shows another method to realize $z_{ctrl}$ using pelvis rotation. The pelvis frame is modified as

$$\boldsymbol{R}_B^{d*} = \boldsymbol{R}_B^d \boldsymbol{R}_{rpy}(\phi_{ctrl}, 0, 0) \quad (21)$$
$$\phi_{ctrl} := z_{ctrl}/w,$$

where $\phi_{ctrl}$ is the amount of pelvis rotation and $w$ is the distance between the right and the left hip joints. By this method, we can control a human-like walking pattern which has moments of fully stretched knee. We use the latter method in the rest of this paper.

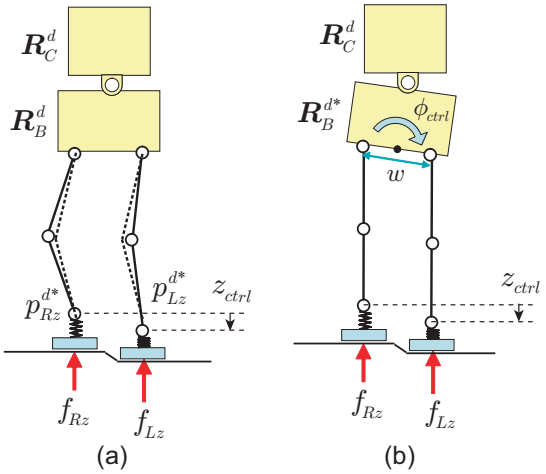


Fig. 7. Foot vertical force distribution

## IV. CoM/ZMP control layer

### A. Ground frame for CoM/ZMP control

To measure the CoM and the ZMP, we introduce a frame whose origin is on the ground and its z-axis is vertical in the world frame. During single support phase, we determine its origin on the sole of support foot and the x-axis to be aligned with the support foot (Fig.8(a)). During double support phase, we set the origin to be the mid point of the soles and the x-axis to be the average of the both foot orientations (Fig.8(b)).

The CoM and ZMP are defined and controlled with respect to this ground frame. We can also calculate the CoM and ZMP trajectories in the world frame by keeping track of the ground frame which jumps at the moment of touchdown and liftoff.

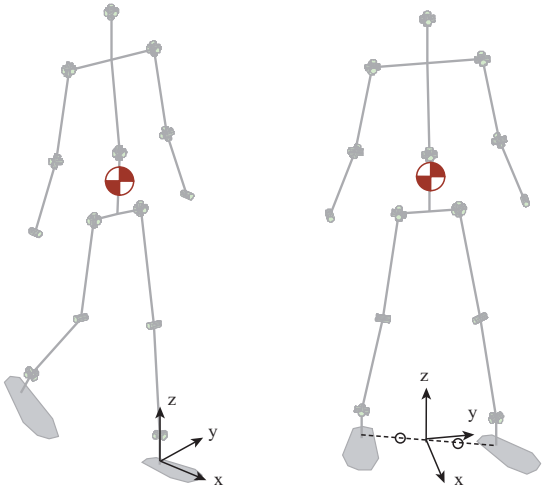


Fig. 8. Frame for CoM/ZMP measurement

### B. Linear Inverted Pendulum Mode

By the posture/force control of the previous section, we can expect that the robot will generate the force specified by the ZMP reference. However, it is unavoidable that the real ZMP lags behind the reference due to the mechanical compliance and the control. To model this effect, we assume following simple dynamics.

$$p = \frac{1}{1 + sT_p} p^d \tag{22}$$

We confirmed that $T_p = 0.05$s gives a good approximation of the ZMP delay by the preliminary experiment.

When we give a walking pattern for standing upright, the CoM of the robot moves freely because of the foot torque control while the upper body keeps upright by the posture controller. We can approximate this CoM dynamics as linear inverted pendulum mode [22].

$$\ddot{x} = \frac{g}{z_c}(x - p) \tag{23}$$

where $x$, $g$, $z_c$ are horizontal CoM position, gravity acceleration, CoM height respectively. Although the CoM height changes in time, we set constant $z_c = 0.87$m as a nominal value since a linear inverted pendulum requires it to be constant.

It is expected that the CoM/ZMP motion can be modeled by (22) and (23) both in the sagittal and lateral plane. To check this, we applied the following control. Having a reference for the CoM and ZMP as $(x^d, p^d)$, the modified reference ZMP $p^{d*}$ is calculated by

$$p^{d*} = p^d - k_p(x - x^d) - k_d\dot{x} - p_{aux}, \tag{24}$$

where $k_p, k_d$ are feedback gains. To obtain a step response data, we add an auxiliary step input $p_{aux}$ of 2cm. Fig.9 is the experimental result. In the upper graph, the bold and red lines show the CoM and ZMP of the experiment respectively. The simulated response using (22) and (23) are plotted by the thin line (CoM) and the broken red line (ZMP). The lower graph shows the CoM speed in the experiment (bold line) and in the simulation (thin line). Both graphs depict a good correspondence between the experiment and the simulation thus the linear inverted pendulum model was justified as the robot dynamics model.

### C. Linear inverted pendulum tracking controller

Let us define a state vector as $\boldsymbol{x} := [x,\ \dot{x},\ p]^T$. The system equation is obtained by combining (22) and (23).

$$\begin{aligned} \frac{d}{dt}\boldsymbol{x} &= \boldsymbol{A}\boldsymbol{x} + \boldsymbol{B}u \\ \boldsymbol{A} &:= \begin{bmatrix} 0 & 1 & 0 \\ g/z_c & 0 & -g/z_c \\ 0 & 0 & -1/T_p \end{bmatrix}, \\ \boldsymbol{B} &:= \begin{bmatrix} 0 \\ 0 \\ 1/T_p \end{bmatrix} \end{aligned} \tag{25}$$

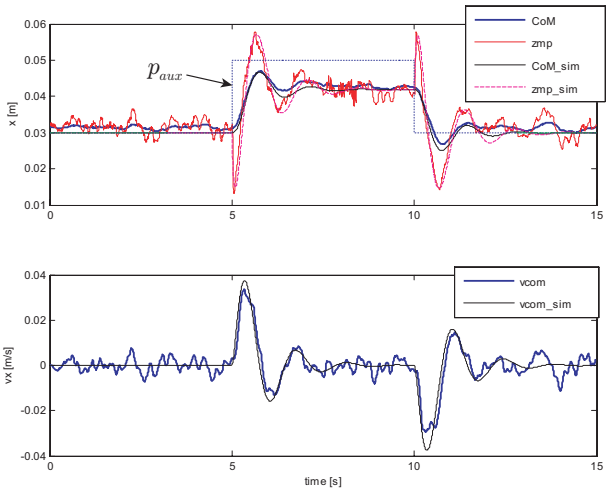


Fig. 9. Step responce of the controlled robot ($k_p = -2.67, k_d = -0.34$)

A walking stabilization can be formalized as tracking of a system state $\boldsymbol{x}$ to a reference state of the walking pattern $\boldsymbol{x}^d$. It is achieved by the following controller.

$$\begin{aligned} u = p^{d*} &= \boldsymbol{K}(\boldsymbol{x}^d - \boldsymbol{x}) + p^d \\ \boldsymbol{K} &:= \begin{bmatrix} k_1 & k_2 & k_3 \end{bmatrix} \end{aligned} \tag{26}$$

where $\boldsymbol{K}$ is a state feedback gain to stabilize (25). Fig.10 shows the block diagram of the proposed tracking controller. When we define the error state as $\Delta\boldsymbol{x} := \boldsymbol{x} - \boldsymbol{x}^d$, its closed

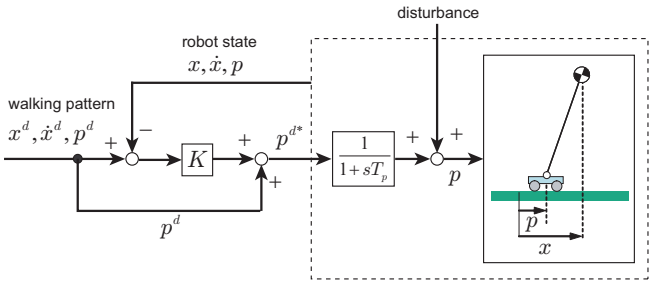


Fig. 10. Linear inverted pendulum tracking controller

loop dynamics is given by

$$\frac{d}{dt}\Delta\boldsymbol{x} = (\boldsymbol{A} - \boldsymbol{B}\boldsymbol{K})\Delta\boldsymbol{x}. \tag{27}$$

The feedback gain is determined by pole assignment for this system. For the experiments of the next section, we assigned the poles as $(-13, -3, -\omega_c)$ in which includes the stable pole of the inverted pendulum $\omega_c := \sqrt{g/z_c}$ to realize the best CoM/ZMP regulator [23].

## V. Experimental Result

### A. Walking

Figure 11 shows HRP-4C walking with a pattern generated by the method of Harada et al. [19]. The CoM and ZMP trajectories of the walking pattern is plotted in the top graph of Fig.12. The middle and the bottom graphs are their time

Fig. 11. Walking HRP-4C

series in sagittal and lateral direction, respectively. The robot steps 0.265m with 1.1s and its average speed is 0.867km/h in the middle of this walking pattern.

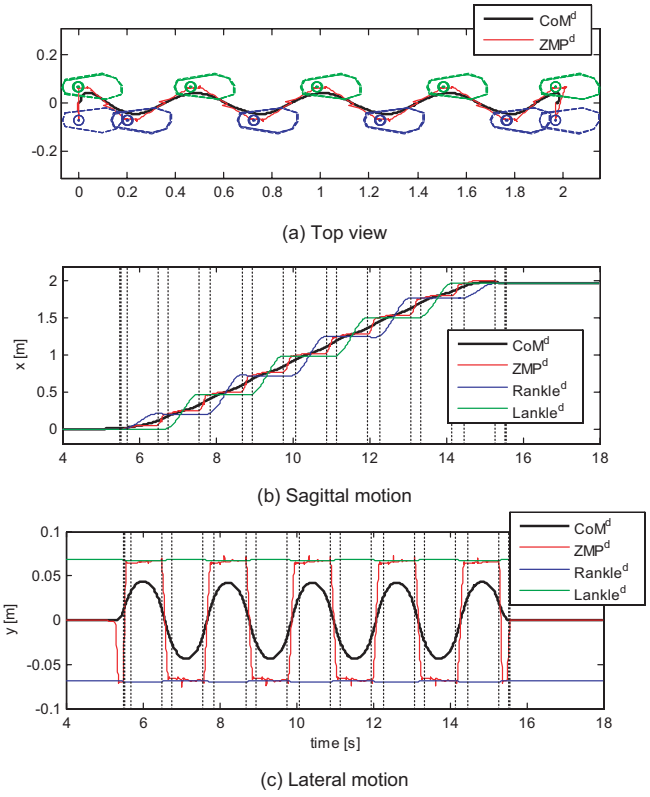


Fig. 12. Walking pattern

The result of walking control is plotted in Fig.13 in the same manner. We observe fluctuation of the ZMP in the lateral direction (the bottom graph) which might be caused by the landing impact or modeling error. Nevertheless, our walking stabilizer could realize a reliable walking so that we could repeat it more than five times.

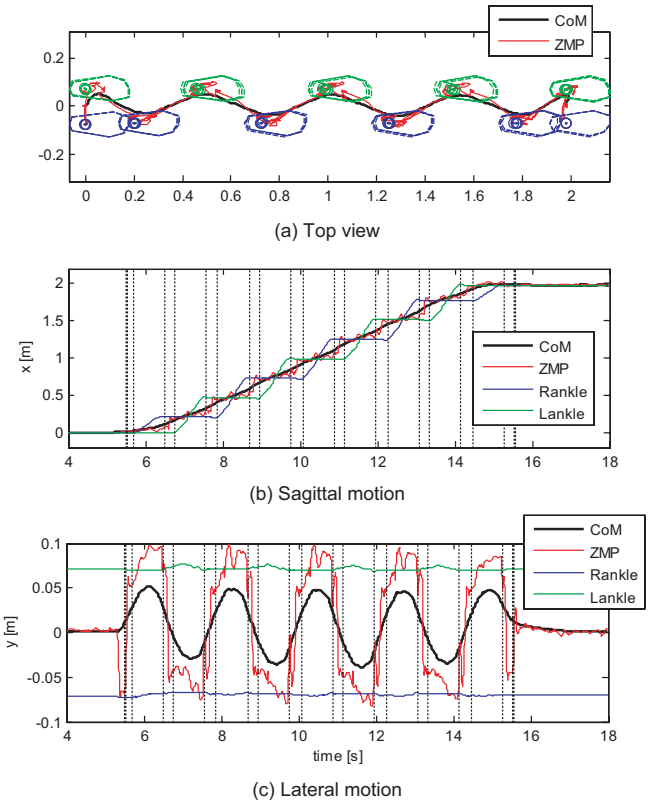


Fig. 13. Realized walking

### B. *Turning motion based on motion capturing*

Fig.14 shows HRP-4C turning 90 degrees in clockwise. In this experiment we used a modified human motion capture data (see Miura et al. [20]).

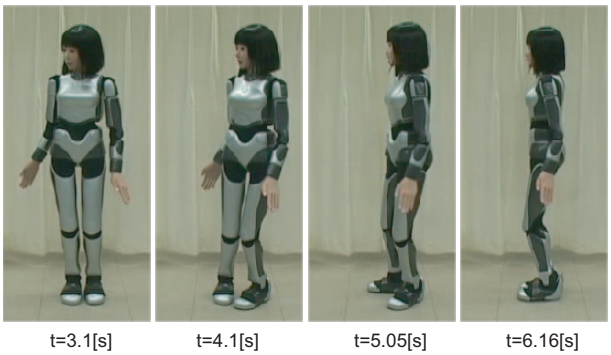


Fig. 14. 90 degree turn based on captured human motion

The CoM/ZMP data of the pattern and the experiment are shown in Fig.15. In the graph, the robot looks right at the beginning and looks bottom after the clockwise turn. The CoM trajectories are plotted by bold black lines and its motion is indicated by arrows. The ZMPs are plotted by red lines. Since there exists a big difference between the CoM/ZMP trajectories, we need further improvement of the controller.

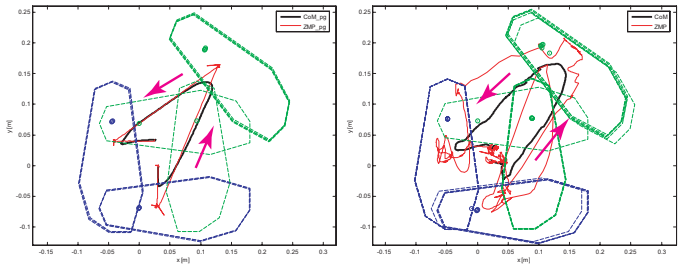

(a) Pattern for 90 degree turn (b) Experimental data of 90 degree turn

Fig. 15. CoM and ZMP while 90 degree turn

Fig.16 shows the results of the posture control. Roll, pitch and yaw angles of the chest link (bold line: experiment, thin line: pattern) and the pelvis link (dashed bold line: experiment, dashed thin line: pattern) are drawn from the top graph to the bottom. We can observe that the chest posture is controlled with good accuracy. On the other hand, the roll and pitch angles of pelvis posture do not track well, because it was modified to control the vertical foot force as explained in III-E.

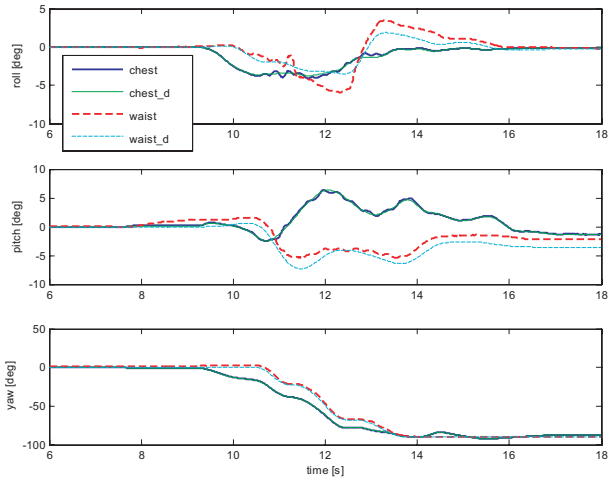


Fig. 16. Posture while 90 degree turn

### C. Outdoor walk

Thanks to the active foot force/torque control, our controller can handle certain ground unevenness. We tested HRP-4C to walk on a pavement whose maximum inclination is 3 degrees using a prescribed walking pattern for a flat ground. The robot could walk without any knowledge of ground profile as shown in Fig.1. The walking speed, the step length and the step time was 0.6km/h, 0.2m and 1.2s, respectively.

Fig.18(a) shows the trajectory of CoM and ZMP in walking direction. After 10s, the robot started to climb a slope of 3 degree. To cope with the slope, the ZMP was modified to remain in the hind leg at each double support phase (shown by red arrows). Fig.18(b) shows ankle pitch control specified by the control law of (17). We can recognize the ground slope at each step, since our controller fits the foot to the ground.

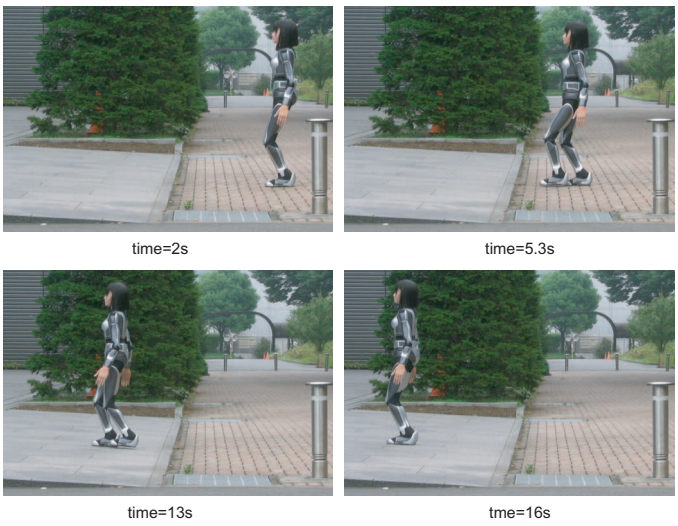


Fig. 17. Walking on a pavement snapshots

## VI. CONCLUSIONS AND FUTURE WORKS

### A. Conclusions

In this paper, we proposed a novel framework of biped walking stabilization control. As the target robot, we used a 42 DOF humanoid robot, cybernetic human HRP-4C which has a body dimensions close to the average Japanese female. We developed a body posture controller and foot force controllers on the joint position servo of the robot. By applying this posture/force control, the robot system could be regarded as a simple linear inverted pendulum with ZMP delay. We confirmed it by a preliminary experiment, and then we introduced a tracking controller design for walking stabilization. The controller was evaluated in the experiments of HRP-4C walking and turning on a floor of our lab. HRP-4C could also perform an outdoor walk on an uneven pavement.

To realize faster and more reliable walk in outdoor, the linear inverted pendulum tracking controller must be improved. Since our formalization well matches the modern control theory, we can expect a great improvement by adopting various methods developed in control engineering community.

## ACKNOWLEDGMENTS

We thank members of humanoid robotics group, Dr.Fujiwara, Dr.Sakaguchi, Dr.Arisumi and Dr.Kita for their technical help and the fruitful discussion with them. We also thank Mr.Ishiwata who developed ART-Linux 2.6, a dependable real-time operating system.

## REFERENCES

[1] M.Vukobratović and J.Stepanenko, "On the Stability of Anthropomorphic Systems," Mathematical Biosciences, vol.15 pp.1-37, 1972.
[2] Collins, S., Ruina, A., Tedrake, R. and Wisse, M., "Efficient Bipedal Robots Based on Passive-Dynamic Walkers," Science, Vol.307, pp.1082-1085, 2005.
[3] Pratt, J., Dilworth, P. and Pratt, G., "Virtual Model Control of a Bipedal Walking Robot," Proc. of the 1997 ICRA, pp.193-198, 1997.

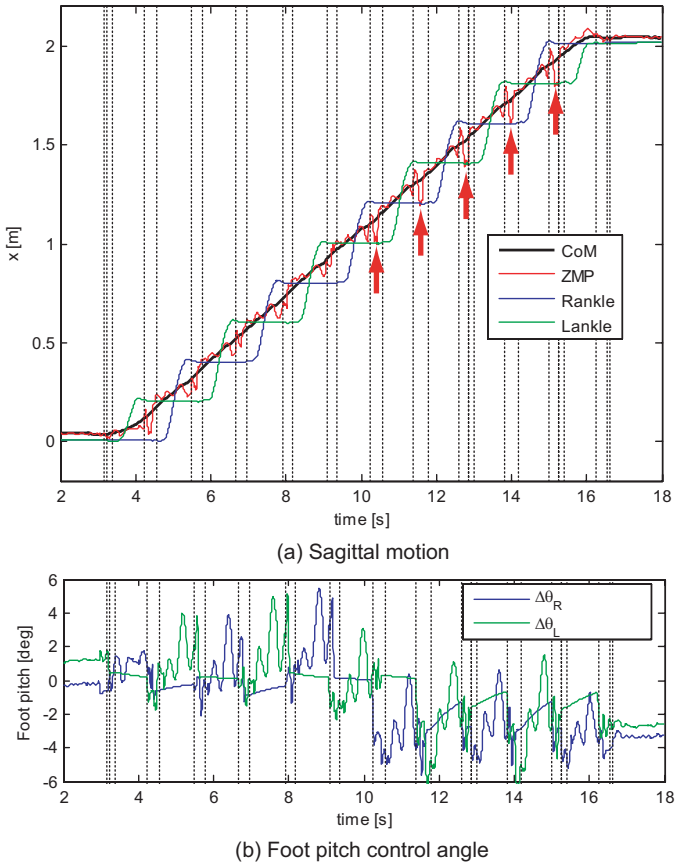


Fig. 18. Control data of the pavement walk


[4] Westervelt, E.R., Grizzle, J.W. and Koditschek, D.E., "Hybrid Zero Dynamics of Planar Biped Walkers," IEEE Trans. on Automatic Control, Vol.48, No.1, pp.42-56, 2003.

[5] K.Nishiwaki and S.Kagami, "High Frequency Walking Pattern Generation based on Preview Control of ZMP," In Proc. of the 2006 IEEE Int. Conf. of Robotics and Automation, pp.2667-2672, 2006.

[6] M.Morisawa, K.Harada et al., "Reactive Stepping to Prevent Falling for Humanoids," In Proc. of 9th IEEE-RAS Conf. on Humanoid Robots, pp.528-534, 2009.

[7] J.Yamaguchi, A.Takanishi and I.Kato, "Experimental Development of a Foot Mechanism with Shock Absorbing Material for Acquisition of Landing Surface Position Information and Stabilization of Dynamic Biped Walking," Proc. of the 1995 IEEE Int. Conference on Robotics and Automation, pp.2892-2899, 1995.

[8] K.Hirai, M.HIrose, Y.Haikawa and T.Takenaka, "The development of Honda Humanoid Robot,", Proc. of the 1998 IEEE Int. Conference on Robotics and Automation, pp.1321-1326, 1998.

[9] K.Nagasaka, M.Inaba and H.Inoue, "Stabilization of Dynamic Walk on a Humanoid Using Torso Position Compliance Control," In Proc. of 17th Annual Conference on Robotics Society of Japan, pp.1193-1194, 1999 (in Japanese)

[10] Y.Choi, D.Kim and B-J.You, "On the Walking Control for Humanoid Robot based on the Kinematic Resolution of CoM Jacobian with Embedded Motion," Proc. of the 2006 IEEE Int. Conf. on Robotics and Automation, pp.2655-2660, 2006.

[11] Q.Huang, K.Kaneko, K.Yokoi et. al, "Balance Control of a Biped Robot Combining Off-line Pattern with Real-time Modification," Proc. of the 2000 IEEE Int. Conf. on Robotics and Automation, pp.3346-3352, 2000.

[12] Jung-Hoon Kim and Jun-Ho Oh, "Walking Control of the Humanoid Platform KHR-1 based on Torque Feedback Control," Proc. of the 2004 IEEE Int. Conference on Robotics and Automation, pp.623-628, 2004.

[13] T.Buschmann, S.Lohmeier and H.Ulbrich, "Biped Walking Control Based on Hybrid Position/Force Control," Proc. of the 2009 IEEE/RSJ Int. Conference on Intelligent Robots and Systems, pp.3019-3024, 2009.

[14] H.Kang, K.Hashimoto, H.Kondo, K.Hattori, K.Nishikawa, Y.Hama, H.Lim, A.Takanishi, K.Suga and K.Kato, "Realization of Biped Walking on Uneven Terrain by New Foot Mechanism Capable of Detecting Ground Surface," Proc. of the 2010 IEEE Int. Conference on Robotics and Automation, pp.5167-5172, 2010.

[15] Koichi Nishiwaki and Satoshi Kagami, "Strategies for Adjusting the ZMP Reference Trajectory for Maintaining Balance in Humanoid Walking," Proc. of the 2010 IEEE Int. Conference on Robotics and Automation, pp.4230-4236, 2010.

[16] K.Kaneko, F.Kanehiro, M.Morisawa, K.Miura, S.Nakaoka and S.Kajita "Cybernetic Human HRP-4C," Proc. IEEE/RSJ Int. Conference on Humanoid Robots, pp.7-14, 2009.

[17] Y.Ishiwata, S.Kagami, K.Nishiwaki and T.Matsui, "ART-Linux 2.6 for Single CPU: Design and Implementation," Journal of the Robotics Society of Japan, vol.26, no.6, pp.546-552, 2008 (in Japanese).

[18] Digital Human Research Center, "ART-Linux (download site)," `http://www.dh.aist.go.jp/en/research/humanoid/ART-Linux/`

[19] K.Harada, K.Miura, M.Morisawa, K.Kaneko et al. "Toward Human-Like Walking Pattern Generator," Proc. IEEE/RSJ Int. Conference on Intelligent Robots and Systems, pp.1071-1077, 2009.

[20] K.Miura, M.Morisawa, S.Nakao,ka, F.Kanehiro, K.Harada, K.Kaneko and S.Kajita, "Robot Motion Remix based on Motion Capture Data — Towards Human-like Locomotions of Humanoid Robots —, " Proc. IEEE-RAS Int. Conference on Humanoid Robots, pp.596-603, 2009.

[21] Sang-Ho Hyon, "Compliant Terrain Adaptation for Biped Humanoids Without Measuring Ground Surface and Contact Forces," IEEE Trans. on Robotics, pp.171-178, 2009.

[22] Kajita, S., Matsumoto, O. and Saigo, M., "Real-time 3D walking pattern generation for a biped robot with telescopic legs," Proc. of the 2001 ICRA, pp.2299-2306, 2001.

[23] Tomomichi Sugihara, "Standing Stabilizability and Stepping Maneuver in Planar Bipedalism based on the Best COM-ZMP Regulator," Proc. IEEE Int. Conference on Robotics and Automation, pp.1966-1971, 2009.